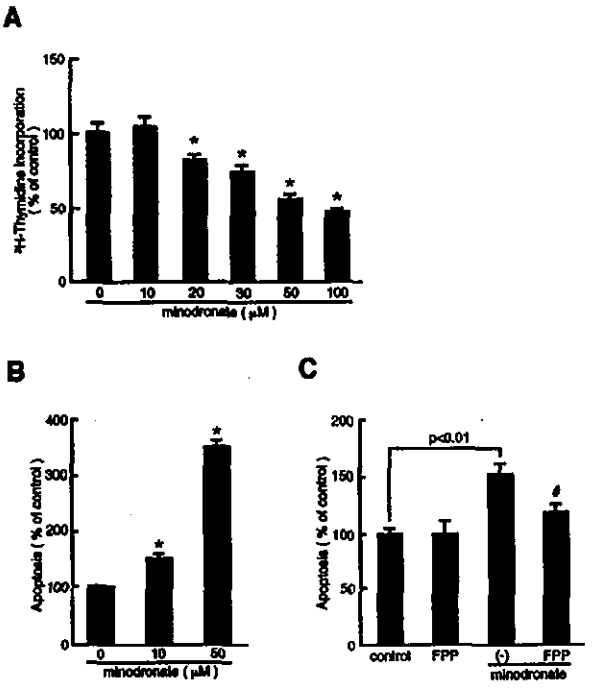

Figure 6. Effects of minodronate on DNA synthesis (**A**) and apoptosis (**B** and **C**) in cultured melanoma cells. G361 melanoma cells were incubated with the indicated concentrations of minodronate in the presence or absence of 0.5 μg/ml of FPP for 24 hours. The percentage of [^{3}H]thymidine incorporation is related to the value of the control. One hundred percent indicates 38,620 cpm. Apoptotic cell death was measured as absorbance at 405 nm. The percentage of apoptotic cell death is related to the value of the control without minodronate. *, $P < 0.01$ compared to the control value. #, $P < 0.01$ compared to the value with 10 μmol/L minodronate alone. $N = 4$ to 6 per group. Similar results were obtained in two independent experiments.

tion, DNA synthesis, and tube formation in cultured ECs were quite strong, whereas those on ROS generation in ECs *in vivo* and tumor angiogenesis were modest. These observations suggest that angiogenic factors other than VEGF could also be involved in tumor angiogenesis in melanoma xenografts.

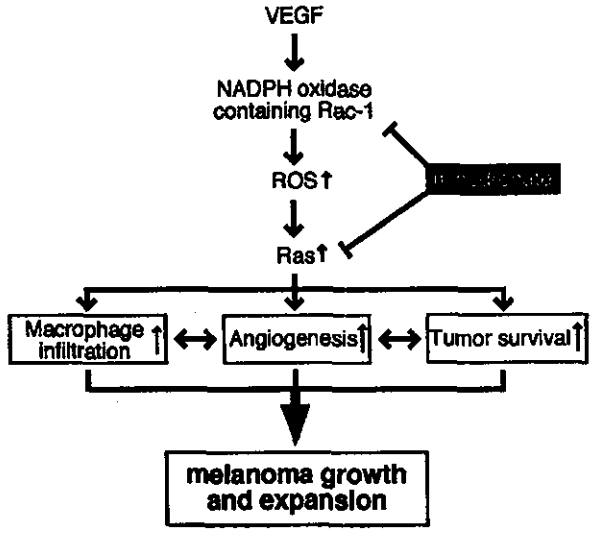

Figure 7. Scheme of possible molecular mechanisms for minodronate-induced growth suppression of melanoma.

It is well known that a number of pathophysiological stimuli induce EC activation as a function of NADPH oxidase-mediated ROS-induced signal transduction.[37] Indeed, NADPH oxidase-derived ROS generation is reported to be required for the angiogenic signaling of VEGF *in vitro*.[15,31] Our present study has extended the previous works. We demonstrated here that geranylgeranylation of Rac, one of the important components of NADPH oxidase, was indispensable for the angiogenic signaling of VEGF and that minodronate blocked the VEGF signaling to angiogenesis by inhibiting NADPH oxidase-mediated ROS generation. Nitrogen-containing bisphosphonates are known to inhibit FPP synthase, thus blocking synthesis of isoprenoid intermediates, FPP and GGPP, which are, respectively, essential for membrane attachment and the biological activity of small G proteins such as Ras and Rac.[11,12,14] These observations suggest that minodronate could block the VEGF signaling in ECs via inhibition of geranylgeranylation of Rac.

In this study, the anti-angiogenic effects of minodronate on VEGF-exposed ECs were not reversed by GGPP. These results suggest that G proteins other than Rac might also be involved in the downstream signaling of VEGF. We obtained the following evidence that Ras was a downstream effector of NADPH oxidase-mediated ROS generation: VEGF activated Ras, which was completely blocked by minodronate or an inhibitor of NADPH oxidase, DPI (Figure 4D); and inactivation of Ras by a farnesyltransferase inhibitor, FTI-276, or overexpression of DN-RasS17N inhibited the angiogenic effects of VEGF on microvascular ECs (Figure 4, E and F). Ras has been proposed as a key regulator of the signaling cascade triggered by oxidative stress,[38–40] and is also required for mitogenic signals of various growth factors including VEGF.[41,42] Taken together, our present study suggests that farnesylation of Ras is also a target of minodronate and that the anti-angiogenic effect of minodronate on VEGF-exposed ECs could be attributed to inhibition of protein prenylation of both Rac and Ras.

VEGF also acts as a proinflammatory cytokine; it not only induces ICAM-1 in ECs, but also stimulates secretion of MCP-1 that recruits leukocytes to sites of inflammation.[33,34] ICAM-1 and MCP-1 are involved in macrophage infiltration into tumors as well, the extent of which is correlated with tumor neovascularization.[43,44] We demonstrated here that minodronate inhibited leukocytes adhesion to VEGF-exposed ECs by suppressing ICAM-1 expression. Further, minodronate inhibited MCP-1 expression both at mRNA and protein levels. Because GGTI-286 or FTI-276, a geranylgeranyltransferase or farnesyltransferase inhibitor, respectively, also inhibited the proinflammatory signals of VEGF (data not shown), minodronate could block the VEGF signaling to inflammation in ECs by inhibiting protein prenylation of both Rac and Ras, as the case in angiogenesis. Although we did not investigate whether minodronate could inhibit peripheral monocyte adhesion to VEGF-exposed ECs, the present study suggests that minodronate could inhibit the tumor-associated macrophage infiltration by suppressing the VEGF signaling to ICAM-1 and MCP-1 overexpression. VEGF has been known to induce expression of ICAM-1

and MCP-1 through the redox-sensitive transcriptional factor, NF-κB activation in ECs.[33,34] Minodronate may inhibit the NF-κB activation induced by VEGF. These observations suggest that the VEGF signaling to inflammation in ECs might also be coupled to the redox state of the cell and that minodronate exerts anti-inflammatory effects on VEGF-exposed ECs through its anti-oxidative properties. Minodronate treatment decreased *in situ* ROS generation in tumor ECs, further supporting our concept that minodronate might block the VEGF signaling *in vivo* through its anti-oxidative properties.

We also found here that minodronate at 10 μmol/L, which effectively blocked the VEGF signaling in cultured ECs, induced apoptotic cell death of cultured G361 cells, whose effects were completely reversed by FPP, but not GGPP (Figure 6C). These results suggest that minodronate acted on melanoma cells directly to induce apoptosis via inhibition of farnesylation of Ras. Essential roles of oncogenic Ras in melanoma genesis and maintenance are reported in mouse models, thus suggesting that pro-apoptotic effects of minodronate observed in our *in vivo* experiments could be attributed partly to its direct effects on melanoma cells.[45]

Taken together, the present study has highlighted two beneficial aspects of the effects of minodronate on melanoma growth and expansion; one is the suppression of tumor-associated angiogenesis and macrophage infiltration probably by blocking the VEGF signaling *in vivo*, and the other is induction of apoptosis in tumor cells. This scenario could possibly explain why the effects of minodronate on tumor growth and survival were extremely impressive, whereas those on tumor angiogenesis were modest.

Our present study provides a novel potential therapeutic efficacy of minodronate for the treatment of melanoma. We do not know whether the other types of nitrogen-containing bisphosphonates have the same anti-tumor effects on melanoma xenografts. Clinical investigation is needed to evaluate the efficacy of this new pharmacological approach as an anti-tumor therapy.

References

1. Holmgren L, O'Reilly MS, Folkman J: Dormancy of micrometastases: balanced proliferation and apoptosis in the presence of angiogenesis suppression. Nat Med 1995, 1:149–153
2. Carmeliet P, Jain RK: Angiogenesis in cancer and other diseases. Nature 2000, 407:249–257
3. Fidler IJ, Ellis LM: The implications of angiogenesis for the biology and therapy of cancer metastasis. Cell 1994, 79:185–188
4. Senger DR, van de Water L, Brown LF, Nagy JA, Yeo KT, Yeo TK, Berse B, Jackman RW, Dvorak AM, Dvorak HF: Vascular permeability factor in tumor biology. Cancer Metastasis Rev 1993, 12:303–324
5. Kim KJ, Li B, Winer J, Armanini M, Gillett N, Phillips HS, Ferrara N: Inhibition of vascular endothelial growth factor-induced angiogenesis suppresses tumor growth in vivo. Nature 1993, 362:841–844
6. Millauer B, Shawve LK, Plate KH, Risau W, Ullrich A: Glioblastoma growth inhibited in vivo by a dominant-negative Flk-1 mutant. Nature 1994, 367:576–579
7. Scappaticci FA: Mechanisms and future directions for angiogenesis-based cancer therapies. J Clin Oncol 2002, 20:3906–3927
8. Brown DL, Robbins R: Developments in the therapeutic applications of bisphosphonates. J Clin Pharmacol 1999, 39:651–660
9. Green JR, Clezardin P: Mechanisms of bisphosphonate effects on osteoclasts, tumor cell growth, and metastasis. Am J Clin Oncol 2002, 25:S3–S9
10. Clezardin P, Fournier P, Boissier S, Peyruchaud O: In vitro and in vivo antitumor effects of bisphosphonates. Curr Med Chem 2003, 10:173–180
11. Van Beek E, Pieterman E, Cohen L, Lowik C, Papapoulos S: Farnesyl pyrophosphate synthase is the molecular target of nitrogen-containing bisphosphonates. Biochem Biophys Res Commun 1999, 264: 108–111
12. Ylitalo R, Kalliovalkama J, Wu X, Kankaanranta H, Salenius JP, Sisto T, Lahteenmaki T, Ylitalo P, Porsti I: Accumulation of bisphosphonates in human artery and their effects on human and rat arterial function in vitro. Pharmacol Toxicol 1998, 83:125–131
13. Fournier P, Boissier S, Filleur S, Guglielmi J, Cabon F, Colombel M, Clezardin P: Bisphosphonates inhibit angiogenesis in vitro and testosterone-stimulated vascular regrowth in the ventral prostate in castrated rats. Cancer Res 2002, 62:6538–6544
14. Okamoto T, Yamagishi S, Inagaki Y, Amano S, Takeuchi M, Kikuchi S, Ohno S, Yoshimura A: Incadronate disodium inhibits advanced glycation end products-induced angiogenesis in vitro. Biochem Biophys Res Commun 2002, 297:419–424
15. Abid MR, Kachra Z, Spokes KC, Aird WC: NADPH oxidase activity is required for endothelial cell proliferation and migration. FEBS Lett 2000, 486:252–256
16. Babior BM: The NADPH oxidase of endothelial cells. IUBMB Life 2000, 50:267–269
17. Egami K, Murohara T, Shimada T, Sasaki K, Shintani S, Sugaya T, Ishii M, Akagi T, Ikeda H, Matsuishi T, Imaizumi T: Role of host angiotensin II type 1 receptor in tumor angiogenesis and growth. J Clin Invest 2003, 112:67–75
18. Torisu H, Ono M, Furue M, Ohmoto Y, Nakayama J, Nishioka Y, Sone S, Kuwano M: Macrophage infiltration correlates with tumor stage and angiogenesis in human malignant melanoma: possible involvement of TNFalpha and IL-1alpha. Int J Cancer 2000, 85:182–188
19. Abe R, Shimizu T, Shibaki A, Nakamura H, Watanabe H, Shimizu H: Toxic epidermal necrolysis and Stevens-Johnson syndrome are induced by soluble Fas ligand. Am J Pathol 2003, 162:1515–1520
20. Yamagishi S, Edelstein D, Du XL, Kaneda Y, Guzman M, Brownlee M: Leptin induces mitochondrial superoxide production and monocyte chemoattractant protein-1 expression in aortic endothelial cells by increasing fatty acid oxidation via protein kinase A. J Biol Chem 2001, 276:25096–25100
21. Miller FJ, Gutterman DD, Rios CD, Heistad DD, Davidson BL: Superoxide production in vascular smooth muscle contributes to oxidative stress and impaired relaxation in atherosclerosis. Circ Res 1998, 82:1298–1235
22. Miyazono K, Okabe T, Urabe A, Takaku F, Heldin CH: Purification and properties of an endothelial cell growth factor from human platelets. J Biol Chem 1987, 262:4098–4103
23. Yamagishi S, Yonekura H, Yamamoto Y, Katsuno K, Sato F, Mita I, Ooka H, Satozawa N, Kawakami T, Nomura M, Yamamoto H: Advanced glycation end products-driven angiogenesis in vitro. Induction of the growth and tube formation of human microvascular endothelial cells through autocrine vascular endothelial growth factor. J Biol Chem 1997, 272:8723–8730
24. Yamagishi S, Inagaki Y, Okamoto T, Amano S, Koga K, Takeuchi M, Makita Z: Advanced glycation end products-induced apoptosis and overexpression of vascular endothelial growth factor and monocyte chemoattractant protein-1 in human cultured mesangial cells. J Biol Chem 2002, 277:20309–20315
25. Nomura M, Yamagishi S, Harada S, Hayashi Y, Yamashima T, Yamashita J, Yamamoto H: Possible participation of autocrine and paracrine vascular endothelial growth factors in hypoxia-induced proliferation of endothelial cells and pericytes. J Biol Chem 1995, 270: 28316–28324
26. de Clerck LS, Bridts CH, Mertens AM, Moens MM, Stevens WJ: Use of fluorescent dyes in the determination of adherence of human leukocytes to endothelial cells and the effect of fluorochromes on cellular function. J Immunol Methods 1994, 172:115–124
27. Sasaki A, Kitamura K, Alcalde RE, Tanaka T, Suzuki A, Etoh Y, Matsumura T: Effect of a newly developed bisphosphonate, YM529, on osteolytic bone metastases in nude mice. Int J Cancer 1998, 77:279–285

28. Ueno T, Toi M, Saji H, Muta M, Bando H, Kuroi K, Koike M, Inadera H, Matsushima K: Significance of macrophage chemoattractant protein-1 in macrophage recruitment, angiogenesis, and survival in human breast cancer. Clin Cancer Res 2000, 6:3282–3289
29. Ohta M, Kitadai Y, Tanaka S, Yoshihara M, Yasui W, Mukaida N, Haruma K, Chayama K: Monocyte chemoattractant protein-1 expression correlates with macrophage infiltration and tumor vascularity in human esophageal squamous cell carcinomas. Int J Cancer 2002, 102:220–224
30. Salven P, Heikkila P, Joensuu H: Enhanced expression of vascular endothelial growth factor in metastatic melanoma. Br J Cancer 1997, 76:930–934
31. Ushio-Fukai M, Tang Y, Fukai T, Dikalov SI, Ma Y, Fujimoto M, Quinn MT, Pagano PJ, Johnson C, Alexander RW: Novel role of gp91phox-containing NAD(P)H oxidase in vascular endothelial growth factor-induced signaling and angiogenesis. Circ Res 2002, 91:1160–1167
32. Weis M, Heeschen C, Glassford AJ, Cooke JP: Statins have biphasic effects on angiogenesis. Circulation 2002, 105:739–745
33. Kim I, Moon SO, Kim SH, Kim HJ, Koh YS, Koh GY: Vascular endothelial growth factor expression of intercellular adhesion molecule 1 (ICAM-1), vascular cell adhesion molecule 1 (VCAM-1), and E-selectin through nuclear factor-κB activation in endothelial cells. J Biol Chem 2001, 276:7614–7620
34. Marumo T, Schini-Kerth VB, Busse R: Vascular endothelial growth factor activates nuclear factor-kappaB and induces monocyte chemoattractant protein-1 in bovine retinal endothelial cells. Diabetes 1999, 48:1131–1137
35. Zhang H, Yano S, Miki T, Goto H, Kanematsu T, Muguruma H, Uehara H, Sone S: A novel bisphosphonate minodronate (YM529) specially inhibits osteolytic bone metastases produced by human small-cell lung cancer cells in NK-cell depleted SCID mice. Clin Exp Metastasis 2003, 20:153–159
36. Yamno S, Zhang H, Hanibuchi M, Miki T, Goto H, Uehara H, Sone S: Combined therapy with a new bisphosphonate, minodronate (YM529), and chemotherapy for multiple organ metastases of small cell lung cancer cells in severe combined immunodeficient mice. Clin Cancer Res 2003, 9:5380–5385
37. Griendling KK, Sorescu D, Ushio-Fukai M: NAD(P)H oxidase: role in cardiovascular biology and disease. Circ Res 2000, 86:494–501
38. Lander HM, Tauras JM, Ogiste JS, Hori O, Moss RA, Schmidt AM: Activation of the receptor for advanced glycation end products triggers a p21(ras)-dependent mitogen-activated protein kinase pathway regulated by oxidant stress. J Biol Chem 1997, 272:17810–17814
39. Aikawa R, Komuro I, Yamazaki T, Zou Y, Kudoh S, Tanaka M, Shiojima I, Hiroi Y, Yazaki Y: Oxidative stress activates extracellular signal-regulated kinases through Src and Ras in cultured cardiac myocytes of neonatal rats. J Clin Invest 1997, 100:1813–1821
40. Irani K, Goldschmidt-Clermont PJ: Ras, superoxide and signal transduction. Biochem Pharmacol 1998, 55:1339–1346
41. van der Geer P, Hunter T, Lindberg RA: Receptor protein-tyrosine kinases and their signal transduction pathways. Annu Rev Cell Biol Chem 1994, 10:251–337
42. Meadows KN, Bryant PB, Pumiglia K: Vascular endothelial growth factor induction of the angiogenic phenotype requires Ras activation. J Biol Chem 2001, 276:49289–49298
43. Becker MD, Kruse FE, Azzam L, Nobiling R, Reichling J, Volcker HE: In vivo significance of ICAM-1-dependent leukocyte adhesion in early corneal angiogenesis. Invest Ophthalmol Vis Sci 1999, 40:612–618
44. Bingle L, Brown NJ, Lewis CE: The role of tumor-associated macrophages in tumor progression: implications for new anticancer therapies. J Pathol 2002, 196:254–265
45. Chin L, Tam A, Pomerantz J, Wong M, Holash J, Bardeesy N, Shen Q, O'Hagan R, Pantginis J, Zhou H, Horner II JW, Cordon-Cardo C, Yancopoulos GD, DePinho RA: Essential role for oncogenic Ras in tumor maintenance. Nature 1999, 400:468–472

CONCISE COMMUNICATION DOI 10.1111/j.1365-2133.2004.06283.X

Detection of 1733insC mutations in an Asian family with Birt–Hogg–Dubé syndrome

H. Kawasaki, D. Sawamura, H. Nakazawa,* N. Hattori,† M. Goto, K.C. Sato-Matsumura, M. Akiyama and H. Shimizu

Department of Dermatology, Hokkaido University Graduate School of Medicine, North 15 West 7, Kita-ku, Sapporo 060-8638, Japan
*Department of Public Health, Sapporo Medical University, Sapporo, Japan
†Department of Dermatology, Faculty of Medicine, University of Tokyo, Tokyo, Japan

Correspondence
Daisuke Sawamura MD.
E-mail: smartdai@med.hokudai.ac.jp

Accepted for publication
5 May 2004

Key words:
1733insC, Asian, cancer syndrome, fibrofolliculoma, tumour suppressor gene

Conflict of interest:
None declared.

Summary

Background Birt–Hogg–Dubé syndrome (BHD) is a rare autosomal dominant genodermatosis characterized by skin tumours, including multiple fibrofolliculomas, trichodiscomas and acrochordons. BHD patients also may suffer from associated renal and colonic carcinomas. The defective gene in BHD has been recently identified and is suspected of being a tumour suppressor gene. Several mutations of the BHD gene have been reported only in Caucasian patients.

Objectives This study reports the first Asian family that has been demonstrated to carry a BHD mutation.

Patients/methods The proband was a 26-year-old Japanese man with multiple asymptomatic, soft skin-coloured papules on his face, neck and trunk, which were clinically thought to be acrochordon. His father was also affected. Histopathologically, the papules revealed a fibrofolliculoma that had a circumscribed proliferation of fibroblasts and collagen fibres surrounding an abnormal hair follicle.

Results Mutational analysis of the BHD gene of the proband and the father detected 1733insC, a cytosine insertion mutation in an eight-cytosine tract (nucleotides 1733–1740) in exon 11. Analysis of fibrofolliculoma in the proband showed heterozygous 1733insC mutation, suggesting the absence of loss of heterozygosity. Interestingly, previous mutational analysis in Caucasian patients revealed that both1733insC and 1733delC mutations were hot spots.

Conclusions This study is the first to find the same hot-spot 1733insC mutation in Asian kindred. The mutations in this polycytosine tract may have a wide, global distribution despite their arising from a different ethnic background.

Birt–Hogg–Dubé syndrome (BHD, OMIM 135150) is a rare autosomal dominant disease characterized by the development of multiple follicular tumours on the face and trunk, which histologically correspond to fibrofolliculomas or trichodiscomas.[1] Additional features include susceptibility to pneumothorax and renal cell carcinoma. Some patients also may suffer from colorectal polyps and cancers. The responsible gene has been mapped to chromosome 17p11.2, recently identified as the BHD gene and shown to encode a 64-kDa protein, folliculin, of unknown function.[2] Germline BHD mutations have been described in 11 Caucasian families and a mutation hotspot at the site of a mononucleotide (eight-cytosine) tract in exon 11 has been identified.[2,3] We encountered a Japanese patient with multiple small skin tumours who was the proband of a BHD family. We finally detected a mutation in the BHD gene in both of the affected members of this pedigree.

Patients and methods

Patients

The proband was a 26-year-old Japanese man, who noticed multiple skin lesions on his face, neck and trunk a year before presentation. Family history revealed that his father had suffered similar skin lesions from the second decade of life while his mother, sister and brother were unaffected (Fig. 1). Examination of the proband revealed multiple, asymptomatic, small, soft, follicular skin-coloured papules found on the patient's face, neck and trunk (Fig. 1A, II-2). Clinically we were initially suspicious of these lesions being common skin tags or acrochordon and took biopsies from a few lesions. Histopathological evaluation of each papule revealed that they basically consisted of aberrant hair follicles circumscribed by

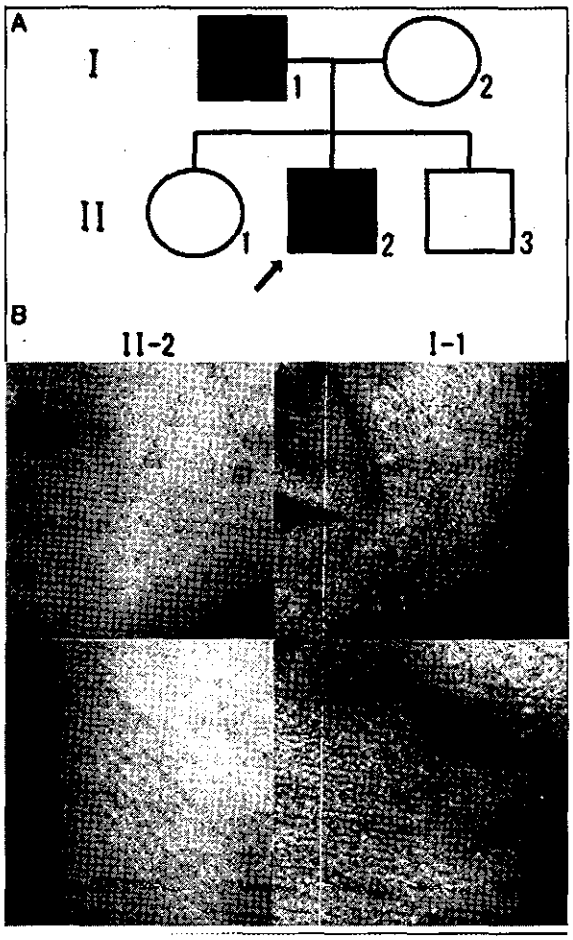

Fig 1. A Japanese family with Birt–Hogg–Dubé syndrome. (A) The family pedigree. The father (I-1) of the proband (II-2) had similar skin lesions while the other members (I-2, II-1 and II-3) were unaffected. (B) Clinical findings show that the proband revealed multiple asymptomatic, small, soft, follicular skin-coloured papules found on the face (a) and neck (b). The father showed a similar clinical phenotype (c,d), but the individual lesions of the father were more severe than those of the proband.

proliferation of fibroblasts and collagen fibres (Fig. 2), compatible with fibrofolliculoma. Afterwards, we performed shave excision of some dozen tumours in accordance with the patient's request and histological findings of all tumours were compatible with fibrofolliculoma. Taking both clinical and histological features together, we finally made a diagnosis of BHD syndrome. We could not find any histological signs of trichodiscoma or acrochordon. His father also had multiple, asymptomatic, small, soft, pedunculated skin-coloured papules on the face, neck and trunk (Fig. 1). The father's lesions were generally harder, larger and more prominent than those of the proband. The father's hair follicle lesions also demonstrated a surrounding proliferation of fibroblast and collagen fibres (data not shown). Past histories of the family members did not show any incidences of neoplasms or pneumothorax.

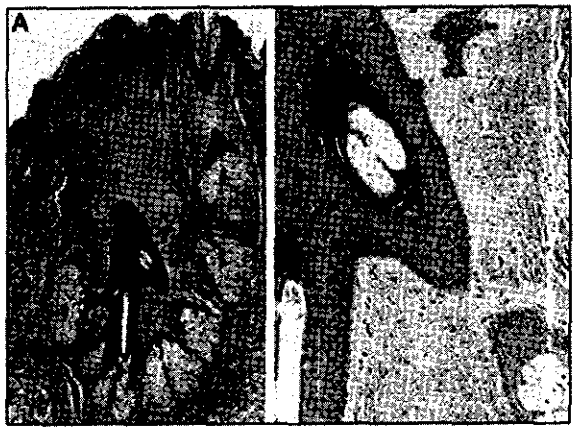

Fig 2. Histological findings. Each papule basically consisted of an aberrant hair follicle (A) and the components of the follicle were circumscribed by proliferation of fibroblasts and collagen fibres (B). Haematoxylin and eosin, original magnification: (A) ×10; (B) ×100.

Mutation analysis

Total genomic DNA was extracted from peripheral blood lymphocytes, and then subjected to mutation screening. The segments of the BHD gene including all 14 exons and all exon–intron borders were amplified by polymerase chain reaction (PCR) using pairs of oligonucleotide primers synthesized in accordance with a previous report.[2] For PCR amplification, approximately 200 ng of genomic DNA, 40 pmol of each primer, 0·5 mmol L^{-1} $MgCl_2$, 20 μmol of each deoxyribonucleoside triphosphate and 1·25 U of Taq polymerase were used in a total volume of 50 μL. The amplification conditions were 94 °C for 5 min, followed by 40 cycles of 94 °C for 45 s, 64 °C for 45 s and 72 °C for 45 s, and extension at 72 °C for 10 min in GeneAmp PCR System 9700 (Perkin Elmer Applied Biosystems, Warrington, U.K.). The PCR products were subjected to automated nucleotide sequencing in an ABI 310 genetic analyser (Perkin Elmer Applied Biosystems).

To determine presence of loss of heterozygosity (LOH), we also excised (but did not microdissect) several large tumours from the proband, removed the normal tissue as much as possible and prepared a DNA sample from each tumour. We examined whether the tumour showed a homozygous pattern of germline mutation.

Results and discussion

In the literature, germline BHD mutations have been detected in only 11 Caucasian families thus far.[2,3] Of these 11 families, five family pedigrees possessed the 1733insC mutation and three families possessed the 1733delC mutation. The remaining three kindreds harboured 1087delAGinsC, 1378 → 1405dup and C1844G mutations. The majority of mutations involve a polycytosine tract (nt 1733–1740) in exon 11, and either deletions or insertions of one cytosine led to the mutations 1733delC and 1733insC, respectively. Indeed, our mutational

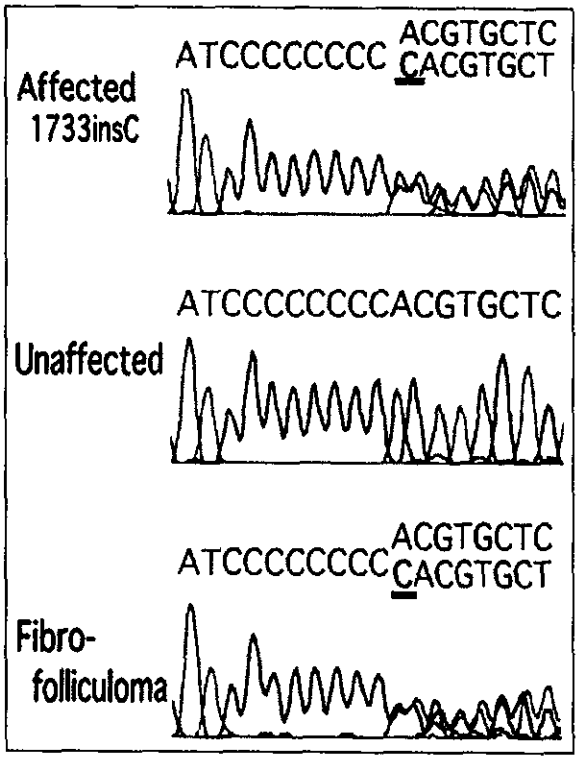

Fig. 3 Detection of the 1733insC mutation in the *BHD* gene. The affected proband and his father showed a cytosine insertion in an eight-cytosine tract (nt 1733–1740) in one allele, resulting in unclear multiple chromatograms after the tract. The unaffected mother and normal controls demonstrated clean waves. DNA samples from several lesions of fibrofolliculoma in the proband also showed heterozygous 1733insC mutation.

analysis of the *BHD* gene of the proband and his father detected heterozygous 1733insC mutation, whereas this mutation was not found in the unaffected mother (Fig. 3). The sister and brother did not consent to DNA analysis. Previous haplotype analysis of BHD families showed a different disease haplotype among the families, suggesting that the hot-spot mutations were not due to a single founder effect but hypermutability of the eight-cytosine tract. Such instability was shown to be a 'slippage' phenomenon during DNA replication in other genes, including *BRCA1*, *NF1* and *APC*.[4–6] This study is the first to find the same hot-spot 1733insC mutation in an Asian kindred and has further confirmed that BHD patients are unlikely to share a single, common ancestor.

BHD syndrome was originally described in 1977 as an inherited genodermatosis characterized by a triad of benign skin tumours consisting of multiple fibrofolliculoma, trichodiscoma and acrochordon. Analysis of the multiple patients suggested an association of this disease with renal and colon carcinomas. However, a large study found no significant risk for the development of colon polyps and cancer, but did find a sevenfold increase risk for renal cancer in BHD patients.[7] Further data accumulation needs to address the association.

Germline mutations in the *BHD* orthologues in the rat and dog indicated these defects were responsible for naturally occurring, inherited renal malignancies in these species.[8,9] The Nihon rat harboured a heterozygous mutation of single cytosine insertion, and the majority of developing renal carcinomas in the rat had the homozygous mutations, indicating LOH at the *BHD* gene.[8] Therefore, it is now known that the BHD syndrome is a hereditary cancer-causing syndrome and that the *BHD* gene might be a tumour suppressor gene. However, evaluation of sporadic renal and colon cancers revealed an inactivated *BHD* gene in a very small proportion of the cases.[10–12] In this study, we analysed DNA samples from several lesions of fibrofolliculoma, and did not find a homozygous 1733insC mutation (Fig. 3), suggesting the absence of LOH.

Because the clinical features of BHD patients include asymptomatic, small, soft, skin-coloured papules, even an experienced clinical dermatologist may misdiagnose this condition as simply acrochordon and might therefore fail to have any chance at detecting the early stages of these forms of cancer. This study suggests that the hot-spot mutation in the polycytosine tract of exon 11 may have a worldwide distribution despite differing ethnic backgrounds.

Finally, we strongly advise that physicians check for *BHD* hot-spot mutations in any patients with widespread acrochordon. Furthermore, physicians should suggest that their patients undergo investigation for kidney and colon lesions when diagnosed with BHD and/or evidence of family history of BHD is indicated.

References

1 Birt AR, Hogg GR, Dube WJ. Multiple fibrofolliculomas with trichodiscomas and acrochordons. *Arch Dermatol* 1977; **113**:1674–7.
2 Nickerson ML, Warren MB, Toro JR *et al.* Mutations in a novel gene lead to kidney tumors, lung wall defects, and benign tumors of the hair follicle in patients with the Birt–Hogg–Dube syndrome. *Cancer Cell* 2002; **2**:157–64.
3 Khoo SK, Giraud S, Kahnoski K *et al.* Clinical and genetic studies of Birt–Hogg–Dube syndrome. *J Med Genet* 2002; **39**:906–12.
4 Rodenhiser D, Chakraborty P, Andrews J *et al.* Heterogenous point mutations in the BRCA1 breast cancer susceptibility gene occur in high frequency at the site of homonucleotide tracts, short repeats and methylatable CpG/CpNpG motifs. *Oncogene* 1996; **12**:2623–9.
5 Rodenhiser DI, Andrews JD, Mancini DN *et al.* Homonucleotide tracts, short repeats and CpG/CpNpG motifs are frequent sites for heterogeneous mutations in the neurofibromatosis type 1 (NF1) tumor-suppressor gene. *Mutat Res* 1997; **373**:185–95.
6 Laken SJ, Petersen GM, Gruber SB *et al.* Familial colorectal cancer in Ashkenazim due to a hypermutable tract in APC. *Nat Genet* 1997; **17**:79–83.
7 Zbar B, Alvord WG, Glenn G *et al.* Risk of renal and colonic neoplasms and spontaneous pneumothorax in the Birt–Hogg–Dube syndrome. *Cancer Epidemiol Biomarkers Prev* 2002; **11**:393–400.
8 Okimoto K, Sakurai J, Kobayashi T *et al.* A germ-line insertion in the Birt–Hogg–Dube (BHD) gene gives rise to the Nihon rat model of inherited renal cancer. *Proc Natl Acad Sci USA* 2004; **101**:2023–7.
9 Lingaas F, Comstock KE, Kirkness EF *et al.* A mutation in the canine BHD gene is associated with hereditary multifocal renal

cystadenocarcinoma and nodular dermatofibrosis in the German Shepherd dog. Hum Mol Genet 2003; 12:3043–53.

10 da Silva NF, Gentle D, Hesson LB et al. Analysis of the Birt–Hogg–Dube (BHD) tumor suppressor gene in sporadic renal cell carcinoma and colorectal cancer. J Med Genet 2003; 40:820–4.

11 Kahnoski K, Khoo SK, Nassif NT et al. Alterations of the Birt–Hogg–Dube gene (BHD) in sporadic colorectal tumors. J Med Genet 2003; 40:511–15.

12 Khoo SK, Kahnoski K, Sugimura J et al. Inactivation of BHD in sporadic renal tumors. Cancer Res 2003; 63:4583–7.

Regular Article for the Journal of Molecular Diagnostics

Epidermolysis bullosa simplex associated with pyloric atresia is a novel clinical subtype caused by mutations in the plectin gene (*PLEC1*)

Hiroyuki Nakamura, Daisuke Sawamura, Maki Goto, Hideki Nakamura, James R. McMillan, Susam Park[1], Sumio Kono[2], Shiro Hasegawa[2], Son'e Paku[3], Tomohiko Nakamura[3], Yoshihumi Ogiso[4], Hiroshi Shimizu*.

Department of Dermatology, Hokkaido University Graduate School of Medicine, Sapporo, Japan, [1]Division of Plastic Surgery and [2]Division of Pediatric Surgery, Shizuoka Children's Hospital, Shizuoka, Japan, and [3]Division of Neonatology and [4]Division of Clinical Pathology, Nagano Children's Hospital, Toyoshina, Japan.

Short title: EBS with PA

***Corresponding author**

Hiroshi Shimizu

Department of Dermatology, Hokkaido University Graduate School of Medicine, North 15, West 7, Sapporo 060-8638, Japan.

Voice: 81-(0)11-706-7387, Fax: 81-(0)11-706-7820

Abbreviations:

BMZ; basement membrane zone, EB: epidermolysis bullosa, EBS; epidermolysis bullosa simplex, EBS-MD; epidermolysis bullosa simplex associated with muscular dystrophy, EBS-PA; epidermolysis bullosa simplex associated with pyloric atresia: HD; hemidesmosome: JEB; junctional epidermolysis bullosa: mAb; monoclonal antibodies.

ABSTRACT

Epidermolysis bullosa (EB) is an inherited mechano-bullous disorder of the skin, and is divided into three major categories, EB simplex (EBS), dystrophic EB and junctional EB (JEB). Mutations in the plectin gene (*PLEC1*) cause EBS associated with muscular dystrophy, whereas JEB associated with pyloric atresia (PA) results from mutations in the α6 and β4 integrin genes. In this study, we examined three EB patients associated with PA from two distinct families. Electron microscopy detected blister formation within the basal keratinocytes leading to the diagnosis of EBS. Surprisingly, immunohistochemical studies using monoclonal antibodies to a range of basement membrane proteins showed that the expression of plectin was absent or markedly attenuated. Sequence analysis demonstrated four novel *PLEC1* mutations. One proband was a compound heterozygote for a nonsense mutation of Q305X and a splice-site mutation of 1344G →A. An exon-trapping experiment suggested that the splice-site mutation induced aberrant splicing of the gene. The second proband harbored a heterozygous maternal nonsense mutation, Q2538X and homozygous nonsense mutations R1189X. Analysis of the intragenic polymorphisms of *PLEC1* suggested that R1189X mutations were due to paternal segmental uniparental isodisomy. These results indicate that *PLEC1* is a possible causative gene in this clinical subtype, EBS associated with PA. Furthermore, two patients out of our three cases died in infancy. In terms of clinical prognosis, this novel subtype is the lethal variant in the EBS category.

INTRODUCTION

Epidermolysis bullosa (EB) comprises a group of genetically determined skin fragility disorders characterized by blistering of the skin and mucous membrane. EB has traditionally been divided into three main categories on the basis of the level of tissue separation within the cutaneous basement membrane zone (BMZ); tissue separations in EB simplex (EBS), dystrophic EB and junctional EB (JEB) occur in the basal keratinocytes, the dermis and the lamina lucida of basement membrane, respectively (Table 1) [1]. Recent advances in EB research, have allowed the identification of mutations in 10 different genes, which account for the clinical heterogeneity in EB (Table 1) [2]. Dominantly inherited EBS results from mutations in the basal keratinocyte-specific keratin 5 and 14 genes, whereas mutations in the plectin gene (*PLEC1*) can cause recessive EBS complicated by muscular dystrophy (EBS-MD). Dystrophic EB is characterized by severe blistering and scarring, and is due to mutations in the type VII collagen gene. The defective genes in JEB include the three genes encoding for the laminin 5 chains, the type XVII collagen gene, or the genes encoding the hemidesmosome-associated integrin α6 and β4 subunits (*ITGA6* and *ITGB4*).

The subtype of JEB involving α6 and β4 integrins is associated with congenital pyloric atresia (PA) [3,4,5]. Staining with specific antibodies to the α6 or β4 integrin subunits in the JEB-PA skin reveals reduced or absent staining [6,7]. JEB-PA is usually lethal, but non-lethal variants have also been reported. The affected individuals with the lethal forms usually die within the first weeks or months after birth, whereas in the non-lethal variants, the clinical severity tends to improve with age [3,5,8,9,10].

However, there have been several recent reports demonstrating EB cases associated with PA showing an

intra-epidermal level of cleavage consistent with the diagnosis of EBS [11,12,13,14]. In this study, we have encountered three similar cases of EBS associated with PA that demonstrated an abnormal epidermal expression of plectin. Furthermore, we have identified novel four mutations, Q305X, 1344G→A, R1189X, Q2538X in the *PLEC1* gene of those cases. Thus, this study furthers our understanding of the possible range of pathophysiology in EB and of the biology of the cutaneous basement membrane.

MATERIALS AND METHODS

Electron Microscopy

For electron microscopic examination, skin specimens were fixed in 5% glutaraldehyde and postfixed in 1% osmium tetroxide, stained en-block in uranyl acetate. They were dehydrated in a graded series of ethanol solutions, then embedded in Araldite 6005. Ultrathin sections were cut, stained with uranyl acetate and lead citrate. The sections were examined with a transmission electron microscope (H-7100; Hitachi, Tokyo, Japan) at 75kv.

Immunofluorescence Studies

Direct immunofluorescence analysis using a series of antibodies against BMZ antigens and cryostat skin sections was performed as described previously [6, 15, 16]. The following monoclonal antibodies (mAbs) against BMZ components were used: mAbs HD1-121, K15, 10F6 and 5B3 against the rod domain of plectin; mAbs GoH3 and 3E1 (Chemicon International, CA) against the α6 and β4 integrins, respectively; mAb GB3 (Sera-lab, Cambridge, UK) against laminin 5 antibody; mAb LH7.2 (Sigma, St. Louis, MO) against type VII collagen; mAb S1193 and HDD20 against BPAG1 and BPA2, respectively. The antibodies GoH3, S1193 and HDD 20 were kind gifts from Dr. Sonnenberg A, the Netherlands Cancer Institute. The antibodies HD1-121 and K15 were kind gifts from Dr. Owaribe K, Nogoya University.

Mutation Detection

Genomic DNA was obtained from both patients and the parents. The mutation detection strategy was performed after polymerase chain reaction (PCR) amplification of all exons and intron-exon borders, followed by direct automated nucleotide sequencing (Applied Biosystems, Foster City, CA). The genomic DNA nucleotides, the cDNA nucleotides and the amino acids of the protein were numbered based on the previous sequence information (GenBank accession no. AH003623) [17]. In particular, PCR amplification of exon 9, 12, 27, and one part of exon 32 was performed using following primers. Primers 5'-GTCGCTGTATGACGCCATGC-3'and 5'-TGGCTGGTAGCTCCATCTCC-3' for exon 9 produced a 387-bp fragment of the genomic DNA extending from g.2717 to g.3103, primers 5'-CCCACTCGCCTTAGGACAGT-3' and 5'-AAACCAACTCTGCCCAAAGC-3' for exon 12 synthesized a 428-bp fragment from g.3571 to g.3998, primers 5'-TTTCGAGGCTGGGGCTTCAT-3' and 5'-GCCTGGGTGATGGTGTGGTC-3' for exon 27 synthesized a 771-pb fragment from g.9681 to g.10451, and primers 5'-TCTGCTTTGGTGGGTGATGG-3'and 5'-AGCCTCTGGTTCTCCTCAGC-3' for a single part of exon 32 synthesized a 422-bp fragment from g.15326-g.15747. The PCR conditions of the amplification were 5 min at 94℃ for one cycle, followed by 38 cycles of 45 s at 94℃, 30 s at 57℃ or 60℃ and 1 min at 72℃. The informed consents for both studies and for publication of the photographs were obtained from the both families in this study.

Verification of Mutations

Each mutation was confirmed by restriction enzyme digestion of PCR products. The Q305X and 1395G->A mutations resulted in the loss of a restriction site for the *PstI* and *HphI*, respectively. The R1189X mutation caused the generation of a

new restriction enzyme site for *Tsp45I*.

There was no proper restriction enzyme to verify the Q2538X mutation. PCR amplification was carried out using the following PCR primers, 5-TCTGCTTTGGTGGGTGATGG-3 and 5-CTCCAGCTTGGCCTTCTCCA-3 for generation of a 225-bp product. We changed the last base of the latter primer (underlined) from the original sequence, so that the combination of this change and the upstream sequence created a new *AluI* site in the PCR product. Since the Q2538X mutation was also located just one base upstream from that primer, Q2538X abolished this *AluI* site.

Exon-Trapping Experiments

Exon trapping system (Invitrogen, Carlsbad, CA) is an approach used for the direct isolation of transcribed sequences from genomic DNA [18]. To generate a *PLEC1* genomic fragment extending from intron 10 to intron 13, we synthesized two primers, 5' -AAACTCGAGGGCTGTCCCAGGTCTGGT-3' and 5' -ATTGGATCCTGGGGCCGTGTGTACCTG-3' which contained the following restriction enzyme sites , *XhoI and BamHI* , respectively. PCR was performed using genomic DNA from the proband 1 as a template. The DNA fragment was digested with *XhoI and BamHI* and subcloned into the multicloning site of a pSPL3 expression vector, which contained a portion of the HIV-1 *tat* gene, an intron, splice donor and acceptor sites, and some flanking exon sequences. Sequence analysis selected constructs with or without the splice site mutation 1344G→A. The constructs were transfected into normal human epidermal keratinocytes using N-[1-(2,3-Dioleoyloxy)propyl]-N,N,N-trimethylammonium methylsulfate (Roche Molecular Biochemicals). Total RNA was extracted from the culture cells and RT-PCR was performed using the trapping vector-specific oligonucleotide primers. The samples without transfection of the pSPL3 were used as controls. The PCR products were subcloned into a TA cloning vector pCR II (Invitrogen) and sequenced.

RESULTS

Clinical Features of EB Associated with PA

The proband 1 was a male, born by spontaneous vaginal delivery at 39 weeks' gestation. His parents were unrelated and clinically normal. Pyloric atresia (PA) and polyhydramnios were suspected antenatally after ultrasound examination. Immediately after delivery, he presented with blisters and widespread ulcers on his trunk, genitalia and legs. Findings from a routine abdominal radiograph led to a clinical diagnosis of EB associated with PA (Fig. 1, A-C). Laparotomy revealed a severely distended stomach with a membrane at the pylorus. The membrane was excised and a pyloroplasty was performed. The histopathology of the septum showed re-epithelization of the epithelium, an atrophic lamina muscularis mucosae, and edematous submucosal tissue. He survived the operation, but still required intensive care at the age of 16 months. His elder brother born 2 years before the proband 1 was also diagnosed as suffering from PA by routine abdominal X-ray. He manifested with multiple blisters and ulcers on his scalp, genitalia, and extremities, identical to those seen in the proband 1 (Fig. 1,D-E). On the second day after birth, pyloroplasty and skin grafting were performed, but he later died of sepsis 4 months after the birth.

The Proband 2 was a female, born by induced vaginal delivery at 36 weeks' gestation, as the second child of non-consanguineous, healthy parents. She had a one-year-old brother who was clinically unaffected. Antenatal ultrasonography had suggested a diagnosis of PA and polyhydramnios. At birth, she presented with blisters and ulcers on the scalp, trunk and extremities (Fig. 2, A-D). Routine abdominal X-rays demonstrated a single abdominal bubble

of gas, resulting in a clinical diagnosis of EB associated with PA. A laparotomy on the second day after birth showed a hugely distended stomach with a membrane at the pylorus. A gastroduodenostomy was subsequently performed. Histopathological analysis of the septum showed atrophic changes in general, normal appearance of the desquamative epithelium, and no increase in collagen fibers numbers. Due to her poor respiratory condition, she died of dyspnea at 31 days of age.

Skin Separation in Basal Keratinocytes

First, we examined the skin separation level within the epidermal BMZ. Electron microscopy of the skin samples from proband 1 revealed that the tissue separation was localized at the base of the basal keratinocytes and that hemidesmosomes (HDs) were reduced in frequency and hypoplastic (Fig. 1F). In the skin sample from the proband 2 there was a reduction in HD numbers and many of the HDs appeared to be small or hypoplastic. The plane of separation was consistently within the basal keratinocyte, just above the HD inner plaque [19]. The majority of HD outer plaques remained attached to the underlying plasma membrane and extracellular electron-dense lamina densa. Keratin filaments within the basal cells appeared to form poor attachment to these rudimentary HDs, which remained firmly attached to the base of the separation (Fig. 2E). The ultrastructural findings in both cases were consistent with these patients being classified as suffering from EBS.

Abnormal Expression of Plectin

An immunohistochemical study using monoclonal antibodies (mAbs) to a range of BMZ component proteins was performed(Fig.3). Immunoreactivity using the mAb HD1-121 against plectin was markedly attenuated in the proband 1 and completely lost in the proband 2. Analysis using other plectin

mAbs K15, 10F6 and 5B5 revealed similar results, in which proband 1 showed markedly reduced expression while no immunoreactivity was detected in the proband 2. Immunostaining for other BMZ proteins including the α6 and β4 integrins, laminin 5, type VII and IV collagens were normal (Fig. 3). BPAG1 and BPAG2 also showed normal, bright, linear labeling of the BMZ in both probands (data not shown).

PLEC1 Mutations in Proband 1

Since abnormal expression of plectin was observed in both probands, we performed direct mutational analysis of the entire plectin gene. In this study, the cDNA nucleotides and the amino acids of the protein were numbered based on the previous sequence information (GenBank accession no. AH003623)(17). Direct nucleotide sequencing of *PLEC1* from proband 1 demonstrated nonsense and splice-site mutations. The nonsense mutation was a C→T transition at nucleotide c.913 of cDNA in exon 9, resulting in the substitution of a glutamine (CAG) at position 305 with a stop codon (TAG) (Q305X). The splice-site mutation was a G→A substitution at nucleotide c.1344 in the cDNA that was located at the 3′ end of exon 12 (1344G→A) (Fig. 4). The Q305X mutation was maternal and the 1344G→A mutation was paternal. These mutations were confirmed by restriction endonuclease analysis (Fig.4).

Since the splice site mutation of 1344G→A might just be a polymorphism, we examined 120 unrelated alleles as control and were unable to detected the same nucleotide change. Furthermore, we performed an exon-trapping experiment, as keratinocytes from the proband 1 or the parents were unavaliable. We inserted the genomic fragments with or without 1344G→A mutation into this vector, transfected these constructs into normal cultured human epidermal keratinocytes and prepared total RNA from the keratinocytes. We then synthesized cDNA, and amplified the extracted exons by PCR. Agarose gel

electrophoresis showed strong 460-bp upper and weak lower 305-bp bands from the samples of the constructs containing the mutation, although a single 554-bp band was amplified from that construct without the mutation (data not shown).

Sequence analysis revealed that the upper 460-bp band contained exons 11 and 13 while the lower 305-bp band contained exon 11 alone. Conversely, exons 11, 12 and 13 were normally extracted from the DNA fragment without the mutation, resulting in a 554-pb band. Deletion of exon 12, which was 94 bp in size, caused a change in the mRNA coding frame and generation of a premature downstream stop codon. However, the combined size of exons 12 and 13 was 249 bp, so the deletion of these exons did not alter the coding frame and restored the translation of a polypeptide that was encoded by the downstream exons.

PLEC1 Mutations in Proband 2

Sequence analysis of the proband 2 revealed an unusual finding of both homozygous and heterozygous mutations. The homozygous mutation was a C→T transition at cDNA position c.3565 in exon 27, resulting in a substitution of an arginine (CGA) at residue 1189 with a stop codon (TGA) (R1189X). Conversely, the heterozygous mutation was a C→T transition at position c.7612 in exon 32, leading to an alteration of a glutamine (CAG) at 2538 to a stop codon (TAG) (Q2538X) (Fig. 6). Nucleotide sequences of her parents disclosed that the father and mother were heterozygous for R1189X and Q2538X, respectively. These mutations were confirmed by restriction endonuclease analysis (Fig. 5).

To eliminate a possibility that a sequence variation under one of the primers caused failure to amplify a maternal allele, we investigated by using a second set of primers for exon 27/intron 28. This also confirmed that the R1189X mutation was homozygous (data not shown).

Furthermore, comparison of 8 intragenic polymorphisms showed that the father and mother were heterozygous for 2/8 and 6/8 markers, respectively (Fig. 6). The mutation R1189X and intron 28/10648 T→A were informative for the absence of a maternal allele in the proband 2. These results indicated that the mutations R1189X and their adjacent sequences were of paternal origin, suggesting possibility of segmental paternal uniparental isodisomy over this short area.

DISCUSSION

Plectin, a component of the hemidesmosome (HD) inner plaque, is involved in the attachment and crosslinking of the cytoskeleton and intermediate filaments to specific membrane complexes [20, 21]. Each monomer comprises a central rod domain of an α-helical coiled-coil structure and flanking amino-and carboxyl-terminal large globular domains [22, 23]. It is widely distributed in almost all tissues and the exact function in each tissue is still unclear [24, 25]. Although a family with EBS Ogna was reported to result from plectin mutation [26], mutations in the plectin gene (*PLEC1*) generally cause EBS associated with muscular dystrophy (EBS-MD), which is characterized by generalized blistering, and a late-onset muscular dystrophy [15,16,17, 27,28,29].

The two probands in this study were both microscopically classified and clinically diagnosed as suffering from EBS associated with PA. We speculated at first, whether the causative mutations might lie in either *ITGA6* or *ITGB4* genes, known to cause PA-JEB. Surprisingly, however, the tissue separation was not within the lamina lucida as might be expected for JEB-PA, but was higher within basal keratinocyte, consistent with EBS. Immunohistochemical examination subsequently revealed abnormal plectin expression, leading us to speculate that mutations in *PLEC1* might be the underlying

cause of this condition.

Indeed, mutational analysis detected novel nonsense and splice-site mutations on each *PLEC1* allele of the first proband (*Fig.* 4). The splice-site mutation is thought to affect the splicing of the *PLEC1* gene, since the G nucleotide in the GT splice donor site in many human genes is relatively conserved within 78 % of all splice junctions [30]. We first examined 120 unrelated alleles and could not detect the same nucleotide change. Furthermore, the exon-trapping experiments revealed that this mutation caused aberrant splicing of this region and suggested that this splice site mutation was likely to be pathogenic.

Immunofluorescence staining using the plectin antibodies, HD1-121, K15, 10F6, and 5B3, detected some plectin expression in proband 1 (Fig.3). HD1-121 recognizes multiple epitopes on the plectin rod domain [31]. In addition, the 10F6 and 5B3 epitopes were located in the central and carboxyl-terminal parts of the rod, respectively [32]. The 1344G →A mutation lies upstream of the region encoding the rod domain. As shown in the exon-trapping experiment, the presence of the low weaker band suggested some expression of the plectin rod domain, which is expected to be insufficient for the normal function of plectin.

Although we found nonsense mutations of both paternal and maternal origins in proband 2, it was unusual that R1189X mutation was homozygous. To further understand the mechanism causing this defect, we searched for several intragenic polymorphisms within the *PLEC1* gene (Fig. 6). The results suggested that the R1189X mutations and their adjacent sequences had originated from one paternal allele. Uniparental disomy refers to the situation in which two copies of a chromosome come from the same parent [33]. The possibility of isodisomy can be hypothesized if two identical segments from one parental homologue are present in the offspring, whereas

sequences of both homologues from the transmitting parent are present in the normal cause, heterodisomy. Angelman syndrome and Prader-Willi syndrome are examples of disorders caused by uniparental disomy [34]. This study indicates that the R1189X mutations and its adjacent sequences are likely to be derived from one paternal homologue and suggested possibility of segmental uniparental paternal isodisomy.

The next point that we should discuss was how *PLEC1* mutation led to PA. We have reviewed the previously reported cases of plectin mutations in EBS-MD. In total, there were 22 mutations, of those 16 mutations resided within the region encoding the rod domain (Fig.7). Out of the 4 novel mutations from our cases, roughly, Q305X, 1344G->A, and Q2538X were not within the rod domain region and R1189X was in the very end of this domain. Plectin interacts with the cytoplasmic tail of β4 integrin via its carboxyl as well as amino-terminal domains (Fig.7) [23, 35], and mutations in the β4 integrin gene result in PA. Therefore, we postulated that the development of PA in our cases is closely linked with the functions of plectin and the β4 integrin subunit. Interestingly, the mutations Q305X and 1344G→A in the first proband resided in the amino-terminal binding site for β4 integrin (Fig.7). However, the mutations of the second proband were not in the β4 integrin binding site.

The level of tissue separation in EBS due to plectin gene mutations is different from that due to K5 or K14 gene mutations. In the latter cases there is a global cytolysis of the basal keratinocytes, while in case of the patients with *PLEC1* mutations the tissue separation is very low at the level of hemidesmosomes. Also, molecular consequences of deletion of the cytoplasmic domain of β4 integrin subunit or the type XVII collagen caused predominant features of EBS with intraepidermal separation [36, 37]. Therefore, some investigators have proposed hemidesmosomal variants that include EBS with muscular dystrophy, JEB with pyloric atresia and generalized atrophic